

Highly-improved lattice field-strength tensor

Sundance O. Bilson-Thompson*, Derek B. Leinweber†, and Anthony G. Williams‡

*CSSM Lattice Collaboration, Special Research Centre for the Subatomic
Structure of Matter and Department of Physics and Mathematical Physics,
University of Adelaide, Adelaide SA 5005, Australia*

(Dated: February 1, 2008)

Abstract

We derive an $\mathcal{O}(a^4)$ -improved lattice version of the continuum field-strength tensor. Discretization errors are reduced via the combination of several clover terms of various sizes, complemented by tadpole improvement. The resulting improved field-strength tensor is used to construct $\mathcal{O}(a^4)$ -improved topological charge and action operators. We compare the values attained by these operators as we cool several configurations to self-duality with a previously defined highly-improved action and assess the relative scale of the remaining discretization errors.

PACS numbers: 12.38.Gc, 11.15.Ha, 12.38.Aw

arXiv:hep-lat/0203008v1 12 Mar 2002

* E-mail: sbilson@physics.adelaide.edu.au

† E-mail: dleinweb@physics.adelaide.edu.au • Tel: +61 8 8303 3423 • Fax: +61 8 8303 3551

WWW: <http://www.physics.adelaide.edu.au/theory/staff/leinweber/>

‡ E-mail: awilliam@physics.adelaide.edu.au • Tel: +61 8 8303 3546 • Fax: +61 8 8303 3551

WWW: <http://www.physics.adelaide.edu.au/theory/staff/williams.html>

I. INTRODUCTION

Lattice gauge theory has shown itself to be an extremely useful tool for studying non-perturbative physics. Its success is founded on the ability to systematically remove errors introduced by the discretization of space-time. The magnitude of such errors are determined by the lattice spacing a . In the continuum limit $a \rightarrow 0$ these error terms vanish, and so one could expect to asymptotically approach continuum physics by moving to finer lattice spacings. Unfortunately the computational cost increases significantly as the spacing decreases.

It is advantageous to ‘improve’ operators by identifying and algebraically eliminating discretization errors from their lattice definitions [1]. In particular, calculations of the Yang-Mills action based upon the strategic combination of several different Wilson loop terms and the reduction of non-classical errors by tadpole improvement [2] have demonstrated a significant decrease in deviations from expected continuum physics in smoothing algorithms such as cooling and smearing (see for instance Ref. [3] and references therein). In this paper we consider the construction of $\mathcal{O}(a^4)$ -improved gluon field-strength tensors, $F_{\mu\nu}$, from which both the topological charge density and the action may be constructed. In the following we refer to such an action as the “reconstructed action”.

The accuracy of our improved operators is investigated by calculating the action, the reconstructed action, and the topological charge on an ensemble of field configurations. We then cool these rough configurations to produce highly self-dual configurations with a range of topological charges. Thermalization and cooling are carried out by use of parallel algorithms with appropriate link partitioning [4]. Comparisons of the topological charge Q , and action normalized to the single-instanton action, S/S_0 , provide quantitative measures of the merit of each of the improvement schemes considered.

This paper is set out as follows: In Section II we look at the lattice definitions of the action and topological charge operators and give a brief discussion of the construction of the $\mathcal{O}(a^4)$ -improved forms of these operators [5]. In Section III we proceed to describe the construction of an analogously improved lattice version of the field-strength tensor, $F_{\mu\nu}$. This tensor is used to construct an improved topological charge operator and the reconstructed action. In Section V we use the cooling of gauge-fields on the lattice to determine which form of improvement gives the most continuum-like results, and compare the standard improved action with the reconstructed action to verify consistency. Our results and conclusions are presented in Section VI.

II. LATTICE ACTION AND TOPOLOGICAL CHARGE

A. Wilson Action

The lattice version of the Yang-Mills action was first proposed by Wilson [6]. The action is calculated from the plaquette, a closed product of four link operators incorporating the

link U_μ ,

$$S_{\text{Wil}} = \beta \sum_x \sum_{\mu < \nu} \left(1 - \frac{1}{N} \text{ReTr} W_{\mu\nu}^{(1 \times 1)} \right), \quad (1)$$

for an $SU(N)$ field theory where the plaquette operator $W_{\mu\nu}^{(1 \times 1)}$ is

$$W_{\mu\nu}^{(1 \times 1)} = U_\mu(x) U_\nu(x + a\hat{\mu}) U_\mu^\dagger(x + a\hat{\nu}) U_\nu^\dagger(x). \quad (2)$$

The link variables $U_\mu(x)$ are defined by the Schwinger line integral

$$U_\mu(x) = \mathcal{P} \exp \left\{ ig \int_x^{x+a\hat{\mu}} dz A_\mu(z) \right\}, \quad (3)$$

and are in general non-Abelian (hence the \mathcal{P} on the right-hand side of Eq. (3) to denote path-ordering). Let us define $W_{\mu\nu}^{(m \times n)}$ to be the closed loop product in the $\mu - \nu$ plane with extent m lattice spacings in the μ -direction and n lattice spacings in the ν -direction. Therefore $W_{\mu\nu}^{(1 \times 1)}$ is the usual plaquette, $W_{\mu\nu}^{(1 \times 2)}$ is an $(a \times 2a)$ loop

$$W_{\mu\nu}^{(1 \times 2)} = U_\mu(x) U_\nu(x + a\hat{\mu}) U_\nu(x + a\hat{\mu} + a\hat{\nu}) U_\mu^\dagger(x + 2a\hat{\nu}) U_\nu^\dagger(x + a\hat{\nu}) U_\nu^\dagger(x), \quad (4)$$

and so on. The Wilson action based on the plaquette for QCD (i.e., $N = 3$) expanded around x_0 , the centre of the plaquette, may be written as follows

$$\begin{aligned} S_{\text{Wil}} &= \beta \sum_{x_0} \sum_{\mu < \nu} \left[1 - \frac{1}{N} \text{ReTr} W_{\mu\nu}^{(1 \times 1)}(x_0) \right], \\ &= \beta \sum_{x_0} \sum_{\mu < \nu} \left[1 - 1 + \frac{a^4 g^2}{6} \text{Tr} F_{\mu\nu}^2(x_0) + \mathcal{O}(g^2 a^6) + \mathcal{O}(g^4 a^6) \right], \\ &= \beta \sum_{x_0} \sum_{\mu < \nu} \left[\frac{a^4 g^2}{6} \text{Tr} F_{\mu\nu}^2(x_0) + \mathcal{O}(g^2 a^6) + \mathcal{O}(g^4 a^6) \right], \\ &= a^4 \sum_{x_0} \sum_{\mu < \nu} \left[\text{Tr} F_{\mu\nu}^2(x_0) + \mathcal{O}(a^2) + \mathcal{O}(g^2 a^2) \right], \quad (\text{setting } \beta = \frac{6}{g^2}), \\ &= a^4 \sum_{x_0} \sum_{\mu, \nu} \left[\frac{1}{2} \text{Tr} F_{\mu\nu}^2(x_0) + \mathcal{O}(a^2) + \mathcal{O}(g^2 a^2) \right], \end{aligned} \quad (5)$$

which reproduces the continuum action to $\mathcal{O}(a^2)$. We note that the path-ordering is crucial to obtaining the non-abelian $F_{\mu\nu} = \partial_\mu A_\nu - \partial_\nu A_\mu + ig[A_\mu, A_\nu]$ with errors of order $\mathcal{O}(g^2 a^2)$.

In this investigation we use cooling to eliminate the high-frequency components of the gauge fields on the lattice. This reveals topological structures which correspond with classical minima of the action. The cooling algorithm works by calculating the local action at each lattice link, and updating the link to minimize this action. However the discretization errors inherent in the Wilson action cause the cooling algorithm to consistently underestimate the action at each lattice link [7]. As a result the link updates do not accurately reflect the true structure of the gauge fields, leading to the destabilization of non-trivial topological structures (instantons and anti-instantons).

B. Improving the Action

The standard Wilson plaquette action, S_{Wil} , contains deviations from the continuum Yang-Mills action of order $\mathcal{O}(a^2)$ and $\mathcal{O}(g^2 a^2)$. This problem may be remedied by improving the action. Tree-level improvement is a simple and effective means of eliminating lowest-order discretization errors by calculating the action from a combination of, for instance, the plaquette, $2a \times a$, and $a \times 2a$ rectangles. Since the plaquette and rectangles have different $\mathcal{O}(a^2)$ errors they may be added in a linear combination in such a way that the leading error terms cancel and one is left with the term corresponding to the Yang-Mills action plus $\mathcal{O}(a^4)$ and $\mathcal{O}(g^2 a^2)$ errors.

The form for a tree-level improved action can be easily determined from the quantities

$$\begin{aligned} \frac{1}{3} \text{ReTr} W_{\mu\nu}^{(1 \times 1)}(x_0) &= 1 - \frac{a^4 g^2}{6} \text{Tr} F_{\mu\nu}^2(x_0) - \frac{a^6 g^2}{72} \text{Tr} F_{\mu\nu}(x_0) (\partial_\mu^2 + \partial_\nu^2) F_{\mu\nu}(x_0) \\ &\quad + \mathcal{O}(g^2 a^8) + \mathcal{O}(g^4 a^6), \end{aligned} \quad (6)$$

$$\begin{aligned} \frac{1}{3} \text{ReTr} W_{\mu\nu}^{(2 \times 1)}(x_0) &= 1 - \frac{4a^4 g^2}{6} \text{Tr} F_{\mu\nu}^2(x_0) - \frac{4a^6 g^2}{72} \text{Tr} F_{\mu\nu}(x_0) (4\partial_\mu^2 + \partial_\nu^2) F_{\mu\nu}(x_0) \\ &\quad + \mathcal{O}(g^2 a^8) + \mathcal{O}(g^4 a^6), \end{aligned} \quad (7)$$

$$\begin{aligned} \frac{1}{3} \text{ReTr} W_{\mu\nu}^{(1 \times 2)}(x_0) &= 1 - \frac{4a^4 g^2}{6} \text{Tr} F_{\mu\nu}^2(x_0) - \frac{4a^6 g^2}{72} \text{Tr} F_{\mu\nu}(x_0) (\partial_\mu^2 + 4\partial_\nu^2) F_{\mu\nu}(x_0) \\ &\quad + \mathcal{O}(g^2 a^8) + \mathcal{O}(g^4 a^6). \end{aligned} \quad (8)$$

Henceforth we shall make use of the definition

$$P_{\mu\nu}^{(m \times n)}(x) \equiv \frac{1}{3} \text{ReTr} W_{\mu\nu}^{(m \times n)}(x). \quad (9)$$

We can therefore readily see that the $\mathcal{O}(a^2)$ terms may be eliminated from the action by making the following construction

$$\begin{aligned} S_{\text{Imp}} &= \frac{5}{3} \beta \sum_x \sum_{\mu < \nu} \left[\left(1 - P_{\mu\nu}^{(1 \times 1)}(x_0)\right) - \frac{1}{20} \left(1 - P_{\mu\nu}^{(2 \times 1)}(x_0)\right) - \frac{1}{20} \left(1 - P_{\mu\nu}^{(1 \times 2)}(x_0)\right) \right], \\ &= a^4 \sum_x \sum_{\mu, \nu} \left[\frac{1}{2} \text{Tr} F_{\mu\nu}^2(x_0) + \mathcal{O}(a^4) + \mathcal{O}(g^2 a^2), \right] \quad \left(\text{setting } \beta = \frac{6}{g^2}\right), \end{aligned}$$

which reproduces the continuum action to $\mathcal{O}(a^4)$ and $\mathcal{O}(g^2 a^2)$.

This process eliminates classical error terms of order $\mathcal{O}(a^2)$ arising from the finite lattice spacing. Non-classical $\mathcal{O}(g^2 a^2)$ errors arising from self-couplings of the gluon fields may be dealt with to some extent by the process of tadpole improvement [2]. Due to the different numbers of links in plaquettes, rectangles, and other possible choices of Wilson loop, one redefines the value of each link by scaling it by the mean link u_0 (to account for the significant tadpole-style self-interactions of the gluon fields introduced on the lattice via the link

operators). In essence u_0 is an estimate of the sum of these unwanted tadpole terms, after the leading $\mathcal{O}(g)$ terms in the links are factored out [2]. Scaling the links by the mean link

$$U_\mu(x) \rightarrow \frac{U_\mu(x)}{u_0}, \quad (10)$$

improves the accuracy of the expansions above. We use the plaquette measure

$$u_0 = \left\langle P_{\mu\nu}^{(1\times 1)}(x) \right\rangle_{x,\mu<\nu}^{\frac{1}{4}}, \quad (11)$$

which is updated after every sweep of cooling. When we include tadpole improvement factors, to correct for the difference between the numbers of links in the plaquette and the rectangular Wilson loops, the improved action takes the long-established form [2]

$$S_{\text{Imp}} = \frac{5}{3}\beta \sum_x \sum_{\mu<\nu} \left[\left(1 - P_{\mu\nu}^{(1\times 1)}(x_0)\right) - \frac{1}{20u_0^2} \left(1 - P_{\mu\nu}^{(2\times 1)}(x_0)\right) - \frac{1}{20u_0^2} \left(1 - P_{\mu\nu}^{(1\times 2)}(x_0)\right) \right]. \quad (12)$$

There is no reason why the tree-level improvement scheme needs to stop at this point. In principle it can be extended to arbitrary orders. For example, de Forcrand *et al.* [5] have used tree-level improvement to construct a lattice action which eliminates $\mathcal{O}(a^4)$ errors, by using combinations of up to five Wilson loop operators. These five loops, which we denote as L_1, \dots, L_5 , have dimensions (1×1) , (1×2) , (2×2) , (1×3) , and (3×3) . Of course, in the case of rectangular loops $m \neq n$ we average the contribution of the loops in each direction. Hence we define

$$\begin{aligned} L_1 &\equiv P_{\mu\nu}^{(1\times 1)}, \\ L_2 &\equiv P_{\mu\nu}^{(2\times 2)}, \\ L_3 &\equiv \frac{1}{2} \left\{ P_{\mu\nu}^{(2\times 1)} + P_{\mu\nu}^{(1\times 2)} \right\}, \\ L_4 &\equiv \frac{1}{2} \left\{ P_{\mu\nu}^{(3\times 1)} + P_{\mu\nu}^{(1\times 3)} \right\}, \\ L_5 &\equiv P_{\mu\nu}^{(3\times 3)}. \end{aligned}$$

The improved action of de Forcrand *et al.* can then be written in the form

$$S = \sum_{i=1}^5 \frac{1}{(m^2 n^2)} c_i S_i, \quad (13)$$

where S_i is the action calculated by inserting the loop L_i in place of $U_{\mu\nu}$ in the definition of the Wilson action, Eq. (1), where m and n are the dimensions of the loop L_i , and where the c_i are improvement constants which control how much each loop contributes to the total improved action. In our work we explicitly include tadpole improvement factors,

$$\frac{1}{u_0^{(2m+2n-4)}}, \quad (14)$$

whereas de Forcrand *et al.* left these factors as unity in Eq. (13). Our experience is that tadpole improvement factors are beneficial in the early stages of cooling and remain

beneficial even as $u_0 \rightarrow 1$.

The values of the improvement constants which eliminate order $\mathcal{O}(a^4)$ tree-level error terms are

$$\begin{aligned} c_1 &= (19 - 55c_5)/9, \\ c_2 &= (1 - 64c_5)/9, \\ c_3 &= (640c_5 - 64)/45, \\ c_4 &= 1/5 - 2c_5, \end{aligned}$$

where c_5 is a free variable. By adjusting c_5 we create different $\mathcal{O}(a^4)$ -improved actions, which in general will have different $\mathcal{O}(a^6)$ error terms. This means that we can attempt to minimize $\mathcal{O}(a^6)$ errors by tuning c_5 . If we set $c_5 = 1/10$, then $c_3 = c_4 = 0$ creating a “3-loop” action, i.e., an action constructed from three of the five loops. Setting $c_5 = 0$ we create a “4-loop” improved action. To construct a specific 5-loop action, de Forcrand *et al.* chose to set $c_5 = 1/20$, halfway between the 3-loop and 4-loop values to stabilize single instanton sizes under cooling. These so-called 3-loop, 4-loop, and 5-loop improved actions are all free of $\mathcal{O}(a^4)$ errors, and have been shown to preserve (anti-)instantons for many thousands of sweeps.

C. Topological Charge

On the lattice, the total topological charge is obtained by summing the charge density

$$q(x) = \frac{g^2}{32\pi^2} \epsilon_{\mu\nu\rho\sigma} \text{Tr}\{F_{\mu\nu}(x)F_{\rho\sigma}(x)\}, \quad (15)$$

over each lattice site

$$Q = \sum_x q(x), \quad (16)$$

where μ, ν, ρ, σ sum over the directions of the lattice axes. Further to their construction of the improved action, de Forcrand *et al.* have used an analogous procedure to define an improved lattice topological charge operator [5]. We choose to construct the $\mathcal{O}(a^4)$ -improved topological charge in a different manner. In the next section we derive an improved version of the field-strength tensor, $F_{\mu\nu}$. This improved operator forms the basis of our definition of the improved topological charge. The derivation of the improved field-strength tensor will serve to illustrate the general methods used to deduce the results already stated (without proof) above for the improved action.

III. THE LATTICE FIELD-STRENGTH TENSOR

Consider the problem of expanding a generic Wilson loop operator. Such an operator is defined as the path-ordered exponential of the closed path integral around the loop

$$W_{\mu\nu}^{(m \times n)} = \mathcal{P} e^{ig \oint A \cdot dx}. \quad (17)$$

As noted earlier, the path ordering is crucial to obtaining the full non-abelian field-strength tensor in the action associated with $W_{\mu\nu}^{(m \times n)}$ such that the errors are $\mathcal{O}(g^2 a^2)$. Note that mean-field improvement reduces the magnitude of these $\mathcal{O}(g^2 a^2)$ errors present early in the cooling process. The $\mathcal{O}(g^2 a^2)$ errors are also suppressed via cooling and we do not consider them further.

We are considering tree-level improvement to remove $\mathcal{O}(a^4)$ and higher errors. It is therefore sufficient to work to leading non-vanishing order in g , which is equivalent to the abelian theory. We hence determine the coefficients in the expansion of any Wilson loop by considering the weak coupling limit $g \rightarrow 0$.

Rewriting the abelian version of the line integral $\oint A \cdot dx$ in Eq. (17) as $\oint (A_\mu dx_\mu + A_\nu dx_\nu)$ we see that we can apply the two-dimensional version of Stoke's theorem (i.e., Green's theorem)

$$\oint_{\partial R} J dx + K dy = \int \int_R \left(\frac{\partial K}{\partial x} - \frac{\partial J}{\partial y} \right) dx dy, \quad (18)$$

where ∂R is the closed contour containing the two-dimensional surface R . Therefore we see that we can readily rewrite our integral around the loop as

$$\oint A \cdot dx = \int_{-ma/2}^{ma/2} dx_\mu \int_{-na/2}^{na/2} dx_\nu (\partial_\mu A_\nu(x_0 + x) - \partial_\nu A_\mu(x_0 + x)). \quad (19)$$

where x_0 is the centre of the loop. The integrand is identified as the abelian field-strength tensor

$$\oint A \cdot dx = \int_{-ma/2}^{ma/2} dx_\mu \int_{-na/2}^{na/2} dx_\nu F_{\mu\nu}(x_0 + x). \quad (20)$$

Hence the expansion of any abelian loop will be in powers of $F_{\mu\nu}$, reproducing the $F_{\mu\nu} F^{\mu\nu}$ term of the action at order $\mathcal{O}(g^2)$, and containing error terms of relative order $\mathcal{O}(g^2 a^2)$ and $\mathcal{O}(a^4)$.

Now we Taylor expand the $F_{\mu\nu}$'s around the point x_0

$$\begin{aligned} \oint A \cdot dx = \int_{-ma/2}^{ma/2} dx_\mu \int_{-na/2}^{na/2} dx_\nu & \left(F_{\mu\nu}(x_0) + \sum_\alpha x_\alpha \partial_\alpha F_{\mu\nu}(x_0) \right. \\ & \left. + \frac{1}{2} \sum_{\alpha,\beta} x_\alpha x_\beta \partial_\alpha \partial_\beta F_{\mu\nu}(x_0) + \dots \right), \end{aligned} \quad (21)$$

Since our plaquette is a two-dimensional object we sum over the μ and ν directions, ($\alpha = \mu$ or ν , and similarly for β).

$$\begin{aligned} \oint A \cdot dx = \int_{-ma/2}^{ma/2} dx_\mu \int_{-na/2}^{na/2} dx_\nu & \left(F_{\mu\nu}(x_0) + \{x_\mu \partial_\mu + x_\nu \partial_\nu\} F_{\mu\nu}(x_0) \right. \\ & + \{x_\mu x_\nu \partial_\mu \partial_\nu\} F_{\mu\nu}(x_0) + \frac{1}{2} \{x_\mu^2 \partial_\mu^2 + x_\nu^2 \partial_\nu^2 + x_\mu^2 x_\nu \partial_\mu^2 \partial_\nu + x_\mu x_\nu^2 \partial_\mu \partial_\nu^2\} F_{\mu\nu}(x_0) \\ & \left. + \frac{1}{6} \{x_\mu^3 \partial_\mu^3 + x_\nu^3 \partial_\nu^3 + x_\mu^3 x_\nu \partial_\mu^3 \partial_\nu + x_\mu x_\nu^3 \partial_\mu \partial_\nu^3\} F_{\mu\nu}(x_0) \right) \end{aligned}$$

$$\begin{aligned}
& + \frac{1}{24} \{x_\mu^4 \partial_\mu^4 + x_\nu^4 \partial_\nu^4\} F_{\mu\nu}(x_0) \\
& + \frac{1}{4} \{x_\mu^2 x_\nu^2 \partial_\mu^2 \partial_\nu^2 + x_\mu^2 x_\nu^2 \partial_\mu^2 \partial_\nu^2\} F_{\mu\nu}(x_0) + \mathcal{O}(x^5). \tag{22}
\end{aligned}$$

The terms with odd powers of x_μ or x_ν vanish upon integration, because of the symmetric integration limits, about the center of the loop. Let us perform the expansion of the standard (1×1) plaquette.

$$\begin{aligned}
\oint A \cdot dx &= \int \int_{-a/2}^{a/2} dx_\mu dx_\nu \left(F_{\mu\nu}(x_0) + \frac{1}{2} \{x_\mu^2 \partial_\mu^2 + x_\nu^2 \partial_\nu^2\} F_{\mu\nu}(x_0) \right. \\
& \quad \left. + \frac{1}{24} \{x_\mu^4 \partial_\mu^4 + x_\nu^4 \partial_\nu^4\} F_{\mu\nu}(x_0) + \frac{1}{4} \{x_\mu^2 x_\nu^2 \partial_\mu^2 \partial_\nu^2 + x_\mu^2 x_\nu^2 \partial_\mu^2 \partial_\nu^2\} F_{\mu\nu}(x_0) + \mathcal{O}(x^5) \right), \\
&= a^2 F_{\mu\nu}(x_0) + \frac{a^4}{24} (\partial_\mu^2 + \partial_\nu^2) F_{\mu\nu}(x_0) \\
& \quad + \frac{a^6}{1920} (\partial_\mu^4 + \partial_\nu^4) F_{\mu\nu}(x_0) + \frac{a^6}{576} (\partial_\mu^2 \partial_\nu^2) F_{\mu\nu}(x_0) + \mathcal{O}(a^8). \tag{23}
\end{aligned}$$

This expansion can be determined to arbitrary order by taking the Taylor expansion in Eq. (21) to the desired order.

So consider again the form taken by the equation for the expansion of the (1×1) loop operator in the non-abelian case, which derives from the Schwinger line integral around a closed path

$$W_{\mu\nu}^{(1 \times 1)} = \mathcal{P} e^{ig \oint A \cdot dx} = \mathcal{P} \left\{ 1 + ig \oint A \cdot dx - \frac{g^2}{2} (\oint A \cdot dx)^2 + \dots \right\}. \tag{24}$$

The standard approach to constructing the action is to take the real part of the trace of this expansion, thereby extracting the leading term which is just one, and the third term which is proportional to $F_{\mu\nu}^2$. However we are interested here in extracting the term proportional to $F_{\mu\nu}$. We can do this by making the following construction, which takes advantage of the hermitian properties of the Gell-Mann matrices

$$\begin{aligned}
W_{\mu\nu}^{(1 \times 1)} &= \mathcal{P} \left\{ 1 + ig \oint A \cdot dx - \frac{g^2}{2} (\oint A \cdot dx)^2 + \mathcal{O}(g^3) \right\}, \\
W_{\mu\nu}^{(1 \times 1)\dagger} &= \mathcal{P} \left\{ 1 - ig \oint A \cdot dx - \frac{g^2}{2} (\oint A \cdot dx)^2 + \mathcal{O}(g^3) \right\},
\end{aligned}$$

and hence

$$\begin{aligned}
\frac{-i}{2} \left[W_{\mu\nu}^{(1 \times 1)} - W_{\mu\nu}^{(1 \times 1)\dagger} - \frac{1}{3} \text{Tr}(W_{\mu\nu}^{(1 \times 1)} - W_{\mu\nu}^{(1 \times 1)\dagger}) \right] &= g \mathcal{P} \oint A \cdot dx + \mathcal{O}(g^3) \\
&= ga^2 \left[F_{\mu\nu}(x_0) + \mathcal{O}(a^2) + \mathcal{O}(g^2 a^2) \right]. \tag{25}
\end{aligned}$$

We have subtracted one-third of the trace to enforce the traceless property of the Gell-Mann matrices.

Eq. (25) demonstrates how we construct the field-strength tensor $F_{\mu\nu}$ from the (1×1) plaquette. Since the expansion in Eq. (23) corresponds with a given Wilson loop only through the choice of integration limits, this suggests that it is also possible to construct an improved field-strength tensor from a suitably chosen linear combination of Wilson loops. This improved field-strength tensor can be fed directly into Eq. (15) resulting in a topological charge which is automatically free of discretization errors to the same order in a^2 . Furthermore, since the Yang-Mills action is based upon the field-strength tensor (squared), it is possible to create a *reconstructed action*, S_R , by inserting the improved field-strength tensor directly into the equation

$$S_R = \beta \sum_x \sum_{\mu, \nu} \frac{1}{2} \text{Tr} F_{\mu\nu}(x)^2. \quad (26)$$

Since the reconstructed action is improved differently to the standard improved action operator, Eq. (13), and constructed from clover terms, the value of the action calculated with the reconstructed action operator can be compared with the value calculated with the standard improved action operator at each cooling sweep as a mechanism to explore the size of the remaining discretization errors.

IV. IMPROVING THE FIELD-STRENGTH

We now wish to construct sums of clover terms designed to remove $\mathcal{O}(a^2)$ and $\mathcal{O}(a^4)$ errors relative to the leading term, $a^2 F_{\mu\nu}$. Let us begin by defining

$$\begin{aligned} \mathcal{A} &= ga^2 F_{\mu\nu}, \\ \mathcal{B} &= ga^4 (\partial_\mu^2 + \partial_\nu^2) F_{\mu\nu}, \\ \mathcal{C} &= ga^6 (\partial_\mu^4 + \partial_\nu^4) F_{\mu\nu}, \\ \mathcal{D} &= ga^6 (\partial_\mu^2 \partial_\nu^2) F_{\mu\nu}. \end{aligned} \quad (27)$$

Let us now denote $C^{(m,n)}$ as the combination of Wilson loop terms extracted from the left-hand-side of Eq. (25) corresponding with the loops used to construct a clover term as depicted in Fig. 1. Constructing the four clover terms and symmetrizing in $n \leftrightarrow m$ we have

$$\begin{aligned} C^{(m,n)} &= \frac{1}{8} \left\{ \int_0^{ma} dx_\mu \int_0^{na} dx_\nu F_{\mu\nu} + \int_{-ma}^0 dx_\mu \int_0^{na} dx_\nu F_{\mu\nu} \right. \\ &\quad + \int_{-ma}^0 dx_\mu \int_{-na}^0 dx_\nu F_{\mu\nu} + \int_0^{ma} dx_\mu \int_{-na}^0 dx_\nu F_{\mu\nu} \\ &\quad + \int_0^{na} dx_\mu \int_0^{ma} dx_\nu F_{\mu\nu} + \int_{-na}^0 dx_\mu \int_0^{ma} dx_\nu F_{\mu\nu} \\ &\quad \left. + \int_{-na}^0 dx_\mu \int_{-ma}^0 dx_\nu F_{\mu\nu} + \int_0^{na} dx_\mu \int_{-ma}^0 dx_\nu F_{\mu\nu} \right\}, \\ &= \frac{1}{8} \left\{ \int_{-ma}^{ma} dx_\mu \int_{-na}^{na} dx_\nu F_{\mu\nu} + \int_{-na}^{na} dx_\mu \int_{-ma}^{ma} dx_\nu F_{\mu\nu} \right\}. \end{aligned} \quad (28)$$

Expanding the loop operators as in Eq. (22) we find that

$$C^{(1,1)} = \mathcal{A} + \frac{1}{6} \mathcal{B} + \frac{1}{120} \mathcal{C} + \frac{1}{36} \mathcal{D},$$

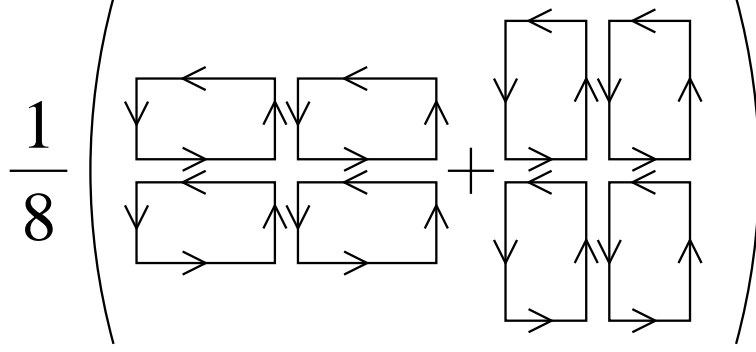


FIG. 1: The four $m \times n$ loops and four $n \times m$ loops used to construct the clover term from which we construct the lattice topological charge operator.

$$\begin{aligned}
C^{(2,2)} &= 4\mathcal{A} + \frac{8}{3}\mathcal{B} + \frac{8}{15}\mathcal{C} + \frac{16}{9}\mathcal{D}, \\
C^{(1,2)} &= 2\mathcal{A} + \frac{5}{6}\mathcal{B} + \frac{17}{120}\mathcal{C} + \frac{2}{9}\mathcal{D}, \\
C^{(1,3)} &= 3\mathcal{A} + \frac{5}{2}\mathcal{B} + \frac{41}{40}\mathcal{C} + \frac{3}{4}\mathcal{D}, \\
C^{(3,3)} &= 9\mathcal{A} + \frac{27}{2}\mathcal{B} + \frac{243}{40}\mathcal{C} + \frac{81}{4}\mathcal{D}.
\end{aligned} \tag{29}$$

Notice that the $\mathcal{O}(a^6)$ terms in each $F_{\mu\nu}$ will be “promoted” to $\mathcal{O}(a^8)$ (and higher) by taking the product $F_{\mu\nu}F_{\rho\sigma}$, while the $\mathcal{O}(a^8)$ terms will be promoted to $\mathcal{O}(a^{10})$ (and higher). Consequently, since we wish to eliminate $\mathcal{O}(a^8)$ errors from the product, we need only expand out to (and eliminate) order $\mathcal{O}(a^6)$ corrections in $F_{\mu\nu}$. We therefore have five equations and four unknowns.

The improved field-strength may be written

$$F_{\mu\nu}^{\text{Imp}} = k_1 C_{\mu\nu}^{(1,1)} + k_2 C_{\mu\nu}^{(2,2)} + k_3 C_{\mu\nu}^{(1,2)} + k_4 C_{\mu\nu}^{(1,3)} + k_5 C_{\mu\nu}^{(3,3)}, \tag{30}$$

where the k_i , the “weightings” of each loop, are defined by

$$\begin{aligned}
k_1 \mathcal{A}^{(1,1)} + k_2 \mathcal{A}^{(2,2)} + k_3 \mathcal{A}^{(1,2)} + k_4 \mathcal{A}^{(1,3)} + k_5 \mathcal{A}^{(3,3)} &= 1, \\
k_1 \mathcal{B}^{(1,1)} + k_2 \mathcal{B}^{(2,2)} + k_3 \mathcal{B}^{(1,2)} + k_4 \mathcal{B}^{(1,3)} + k_5 \mathcal{B}^{(3,3)} &= 0, \\
k_1 \mathcal{C}^{(1,1)} + k_2 \mathcal{C}^{(2,2)} + k_3 \mathcal{C}^{(1,2)} + k_4 \mathcal{C}^{(1,3)} + k_5 \mathcal{C}^{(3,3)} &= 0, \\
k_1 \mathcal{D}^{(1,1)} + k_2 \mathcal{D}^{(2,2)} + k_3 \mathcal{D}^{(1,2)} + k_4 \mathcal{D}^{(1,3)} + k_5 \mathcal{D}^{(3,3)} &= 0,
\end{aligned} \tag{31}$$

such that the weighted coefficient of $ga^2 F_{\mu\nu}$ is 1 and the weighted coefficients of the $\mathcal{O}(a^2)$ and $\mathcal{O}(a^4)$ terms vanish in the sum of loops. Here $\mathcal{A}^{(m,n)}$ represents the coefficient of the \mathcal{A} term from the expansion of $C_{\mu\nu}^{(m,n)}$ and so forth, with the values of the coefficients taken

from Eqs. (29). To find the values of the improvement constants we use these coefficients to construct an equivalent matrix equation. Eq. (31) takes the form

$$\begin{bmatrix} 1 & 4 & 2 & 3 & 9 \\ \frac{1}{6} & \frac{8}{3} & \frac{5}{6} & \frac{5}{2} & \frac{27}{2} \\ \frac{1}{120} & \frac{8}{15} & \frac{17}{120} & \frac{41}{40} & \frac{243}{40} \\ \frac{1}{36} & \frac{16}{9} & \frac{2}{9} & \frac{3}{4} & \frac{81}{4} \end{bmatrix} \begin{bmatrix} k_1 \\ k_2 \\ k_3 \\ k_4 \\ k_5 \end{bmatrix} = \begin{bmatrix} 1 \\ 0 \\ 0 \\ 0 \end{bmatrix}. \quad (32)$$

Using Gauss-Jordan elimination, the improvement coefficients are

$$\begin{aligned} k_1 &= 19/9 - 55k_5, \\ k_2 &= 1/36 - 16k_5, \\ k_3 &= 64k_5 - 32/45, \\ k_4 &= 1/15 - 6k_5, \end{aligned}$$

where the coefficient of the 3×3 loop (in this case k_5) is a tunable free parameter.

We can see that if we set $k_5 = 1/90$, then $k_3 = k_4 = 0$, eliminating the contribution from the $C^{(1,2)}$ and $C^{(1,3)}$ loops and creating a 3-loop $\mathcal{O}(a^4)$ -improved field-strength tensor. We may create a 4-loop improved field-strength tensor in three different ways, by setting $k_5 = 0$, $k_5 = 19/495$, or $k_5 = 1/576$, where the 3×3 , 1×1 or 2×2 loops are eliminated respectively. We focus on a 4-loop improved tensor with $k_5 = 0$ throughout this investigation, analogous to the 4-loop action of de Forcrand *et al.*

It must, of course, be noted that the 3-loop and 4-loop action and field-strength operators are simply special cases of the 5-loop operators, corresponding with particular choices of the parameters c_5 and k_5 respectively for the action and field-strength tensor. As noted above, we have already chosen to investigate a 5-loop action by using de Forcrand *et al.*'s choice of $c_5 = 1/20$, halfway between the 3-loop and 4-loop values of c_5 . In an analogous manner we select the value $k_5 = 1/180$ (midway between the 3-loop and 4-loop values) for the 5-loop improved field-strength tensor.

V. COMPARISON OF IMPROVEMENT SCHEMES

The configurations used in this work are constructed using the Cabbibo-Marinari [8] pseudo-heatbath algorithm with three diagonal $SU(2)$ subgroups looped over twice. We thermalize for 5000 sweeps with an $\mathcal{O}(a^2)$ -improved action with tadpole improvement from a cold start (all links set to the identity) and select configurations every 500 sweeps thereafter. Cooling proceeds via updates of the three diagonal $SU(2)$ subgroups, looped over twice [3]. Configurations are numbered consecutively in the order that they were saved during the process of thermalization. Hence configuration 1 was saved after 5000 thermalization sweeps from a cold start, configuration 2 was saved 500 sweeps after configuration 1, configuration 3 was saved 500 sweeps after configuration 2, and so on. Our results are generated on a

$12^3 \times 24$ (untwisted) periodic lattice at $\beta = 4.60$, with a lattice spacing of $a = 0.125$ fm.

As a thermalized configuration is cooled over the course of many hundreds of sweeps, the action of the configuration monotonically decreases. This occurs because the cooling algorithm smooths out short-range fluctuations in the field. As these ultraviolet components of the field are suppressed, the underlying medium and long-distance structure of the field is revealed. When there are no regions of positive and negative topological charge density in the process of annihilating, the configuration can be thought of as becoming a dilute instanton gas. If cooling proceeds for long enough, the only non-trivial parts of the field which will remain are instantons or anti-instantons.

The total action and topological charge of a configuration satisfy the condition [9]

$$S \geq |Q|S_0 = |Q|\frac{8\pi^2}{g^2}. \quad (33)$$

Since all continuum single (anti-)instantons are non-trivial minima of the local action with $|Q| = 1$, they saturate the equality in Eq. (33) and therefore have an associated action of $S_0 = 8\pi^2/g^2$. For well-cooled configurations it follows that we may estimate the number of instantons on the lattice by dividing the total action by the quantity $S_0 = 8\pi^2/g^2$. We shall see that one of the principal criteria by which we may judge the value of an improvement scheme is how closely the values of S/S_0 and the topological charge approach integer values as we continue cooling and approach self-duality.

In a sufficiently dilute instanton gas the only contributions to the action and topological charge of the field will be that due to the (anti-)instantons. Hence if there are n_I instantons and n_A anti-instantons well-separated on a large volume, the total action and topological charge should be integers, and satisfy the conditions $S/S_0 = n_I + n_A$ and $Q = n_I - n_A$. As cooling proceeds, instanton-anti-instanton pairs will annihilate until $S/S_0 = |Q|$ at which point the configuration is self-dual. What we expect to see is that as we begin cooling, Q should relatively quickly become integer and remain stable thereafter. As we continue to cool towards self-duality we should then see S/S_0 monotonically decreasing to the point where $S/S_0 \rightarrow |Q|$ from above.

Our lattice volume is not large enough that we observe configurations, stable under cooling, with both instantons and anti-instantons simultaneously, i.e., on our lattice they annihilate as cooling proceeds. In Fig. 2 we present the action for two configurations each having a topological charge (stabilized after preliminary cooling) of $|Q| = 1$. As cooling proceeds one observes that S/S_0 repeatedly decreases by an increment of two. During this period the topological charge remains stable. This indicates that the action is dropping due to instanton-anti-instanton annihilation events. Notice that the plateaus persist for longer as cooling continues. It is known that there can be no fully self-dual $|Q| = 1$ configurations on the torus [10, 11]. The fate of $|Q| = 1$ configurations under continued cooling will be discussed elsewhere [12]. We have observed that configurations which stabilize at larger topological charges do not exhibit such pronounced plateauing. It is reasonable to deduce that as the lattice becomes more sparsely populated, the mean period between instanton-anti-instanton annihilation events becomes longer, as it becomes

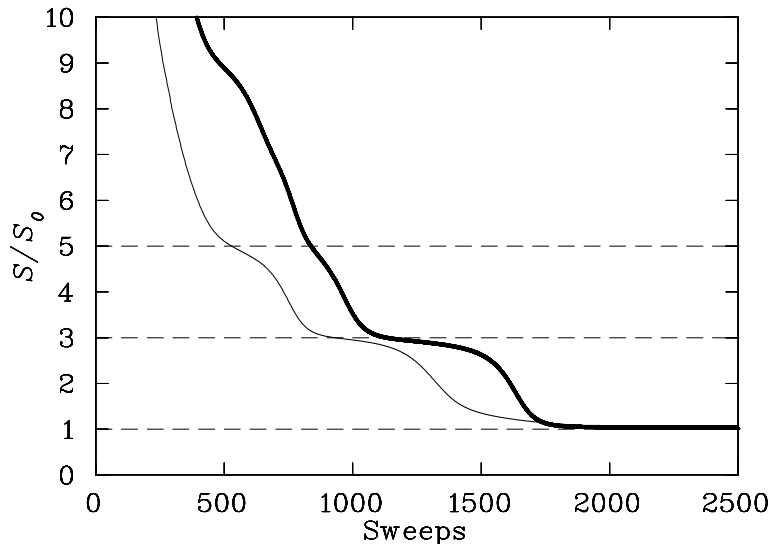


FIG. 2: Action values of configuration 1 (thin line) and configuration 11 (bold line), cooled with the 3-loop improved action. Both configurations have a total topological charge of 1. It can be clearly seen that the action of each configuration repeatedly plateaus briefly near integer values (dashed lines) before dropping by two units. This is characteristic of instanton-anti-instanton annihilation events. In the case of configuration 11, plateauing begins around sweep 500 ($S/S_0 \approx 9$).

possible to have well-separated, weakly-interacting instantons and anti-instantons on the lattice. On a sufficiently large lattice, for sufficiently small total $|Q|$ it should then be possible to arbitrarily closely approach a true dilute instanton gas with both instantons and anti-instantons, where the configuration is locally (but not globally) self-dual.

On the lattice, discretization errors are expected to lead to non-integer values of S/S_0 and topological charge for a highly-cooled configuration. The better the improvement, the closer these values will come to integers. Fig. 3 shows how S/S_0 and the topological charge approach the same value, indicating the approach to a self-dual configuration. They remain stable for several hundred sweeps of improved cooling. We now wish to determine which cooling scheme (3-loop, 4-loop, or 5-loop) and which field-strength improvement scheme are best.

Throughout the discussion of our results we shall use the following notation: the cooling action will be denoted by S , the reconstructed action by S_R and our highly-improved topological charge by Q . In some cases the type of improvement scheme used will be denoted by a number in parentheses. Hence the 3-loop improved cooling action is written as $S(3)$, our topological charge calculated from a 4-loop improved field-strength tensor is written as $Q(4)$, our 5-loop reconstructed action is written as $S_R(5)$, and so on.

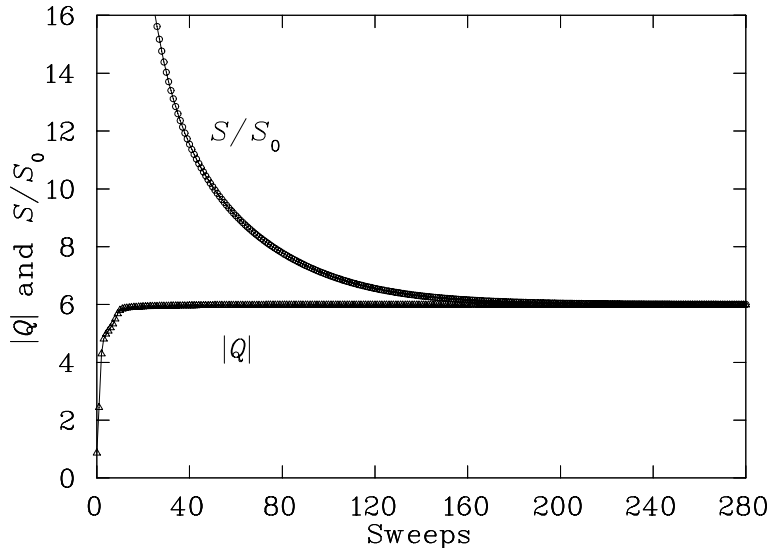


FIG. 3: An example plot of how improved cooling stabilizes the action (circles) and topological charge (triangles) at consistent values. The action is rescaled by dividing by S_0 , the action of a single instanton. Cooling is performed with an $S(3)$ action, and the topological charge is $Q(3)$. [The notation used is that $S(n)$, $S_R(n)$, and $Q(n)$ are the n -loop forms of the improved action, our reconstructed action, and our improved topological charge operator respectively.]

A. Improved Cooling

We shall commence the assessment of which improved action has the smallest discretization errors by demonstrating explicitly the discretization errors in the standard Wilson (plaquette) action. Fig. 4 shows the action against sweep number for a configuration cooled with the Wilson action (triangles), denoted as $S(1)$, and the $S(2)$ action (circles) from Eq. (12). It can be clearly seen that the Wilson action drops to a temporary plateau, but eventually destabilizes and drops by approximately one unit around sweep number 250, and again around sweep number 750. It should also be noted that when the numerical data are examined closely these plateaus are found to occur somewhat below integer values. However the $S(2)$ cooling scheme plateaus at a value much closer to integer (in this case 6) and remains at this value without destabilizing after 1000 cooling sweeps.

This result (and other similar results on other configurations) are an indication that the ordinary Wilson plaquette action significantly underestimates the true action of the configuration. Because the large discretization errors in the action prevent the cooling algorithm from updating the links in a manner which accurately reflects the classical structure of the fields, plaquette cooling destroys important topological structures. It is true that the action may be expected to drop (while the topological charge remains constant) due to instanton-anti-instanton annihilation during the cooling process. However, since the action drops by an increment of one unit (not two) it is clear that we are not observing a decrease in the action as a result of instanton-anti-instanton annihilation, but

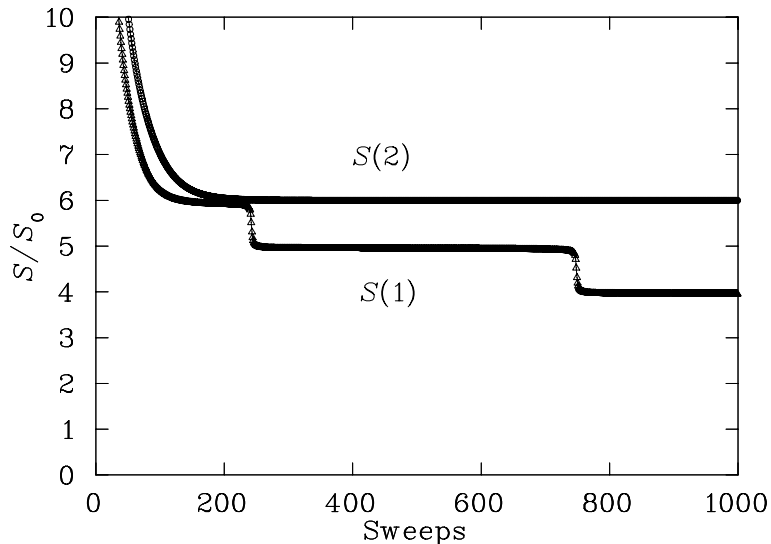


FIG. 4: Action of configuration 89 cooled with $S(1)$ (triangles) and $S(2)$ (circles) cooling schemes after 1000 sweeps. [See Fig. (3) caption for notation.]

rather the destabilization and destruction of a single instanton or anti-instanton.

While the $S(2)$ results are promising, it has already been shown analytically that $S(2)$ does not stabilize instantons on the lattice [7]. Removal of $\mathcal{O}(a^4)$ errors and long-term stabilization of instantons requires the consideration of additional loops.

We now shift our attention to comparisons between the various improved actions. Figs. 5 and 6 show the value of the action attained by two different initial hot configurations as they are cooled with various improved actions. We can see that in both cases the $S(2)$ action plateaus well below the relevant integer value, due to large $\mathcal{O}(a^4)$ discretization errors with negative sign. We furthermore notice that in the case of Fig. 5, the $S(4)$ action drops below the integer plateau at $S/S_0 = 6$. In fact, while not shown here it continues falling to a plateau at $S/S_0 = 5$, indicating that it cools away an instanton-like structure which the other actions do not. When we examine Fig. 6 we see that the discretization errors in the $S(4)$ action are relatively large and have negative sign. This suggests that the $S(4)$ action consistently underestimates the action of the configuration to which it is applied. In the case of Fig. 5 this underestimation was severe enough to completely destroy an instanton during the cooling process. This in itself is quite a remarkable result, since it demonstrates that $\mathcal{O}(a^6)$ discretization errors can be large enough to destabilize instantons in some cases. We shall henceforth discard $S(4)$ cooling on the basis that it has large $\mathcal{O}(a^6)$ discretization errors with negative sign.

B. Improved Topological Charge and Reconstructed Action

In order to determine which improvement scheme for $F_{\mu\nu}$ produces the most continuum-like results we will assess which topological charge operator produces results closest to integer values. The top diagram of Fig. 7 shows the development of the topological charge of a hot configuration over the course of 2400 cooling sweeps with the $S(3)$ improved cooling action. The $Q(1)$ topological charge is too far from an integer value to be seen on the scale we have chosen for this diagram, but we can clearly see that the $Q(3)$ and $Q(4)$ operators produce significantly better results than the $Q(2)$ operator. At the bottom we see equivalent results for configuration 89 (used in Fig. 5), over 1200 sweeps. This time we see that the $Q(3)$ operator gives marginally more integer-like results than those observed with the $Q(4)$ operator. But again the $Q(1)$ and $Q(2)$ operators are substantially more inaccurate, as we would expect from the order of improvement used to construct $Q(3)$ and $Q(4)$. Our $Q(5)$ operator, constructed with a value of k_5 midway between the 3-loop and 4-loop values, produces near-perfect results for both parts of Fig. 7, sitting between the $Q(3)$ and $Q(4)$ values. Further fine tuning of k_5 appears unnecessary as $Q(5)$ lies above and below the integer values in the top and bottom plots of Fig. 7 respectively.

Since the improved field-strength tensor plays no role in affecting the structure of the field configurations as they cool, we consider an ensemble of configurations that have already been cooled to self-duality (for several hundred sweeps) and assess their topological charge (and reconstructed action) with each different improved $F_{\mu\nu}$. Table I shows these results for a number of configurations, all $S(3)$ cooled. We can see that in three of the four cases the 5-loop improved topological charge, $Q(5)$, and reconstructed action, $S_R(5)$, produce results that are both closest to integer values, and in closest agreement to the value of the cooling action. In the case of configuration 56, $S_R(3)$ and $Q(3)$ produce the results closest to integer values.

A further comparison, between results for $S(3)$ and $S(5)$ cooling, is presented in Table II. In this case we wish to determine whether the choice of cooling action affects the dependability of the reconstructed action. We have not chosen to consider the $S(4)$ cooling as it has already been deemed unreliable. We see that in the later stages of cooling, $S_R(5)$ gives values closer to the cooling action used in each case (whether the cooling action is 3-loop or 5-loop), which suggests that it may be a more accurate probe of the structure of the fields produced by the cooling algorithm than either the 3-loop or 4-loop reconstructed action operators. For these reasons it appears that the 5-loop improved field-strength tensor with $k_5 = 1/180$ is the most dependable of the choices we have examined.

VI. DISCUSSION

We have now considered the relative merits of the various improvement schemes for the cooling action. We have also considered the relative merits of the various improvement schemes for the reconstructed action and the topological charge operators (which of course are indicative of the accuracy of the improved field-strength tensor). It appears that

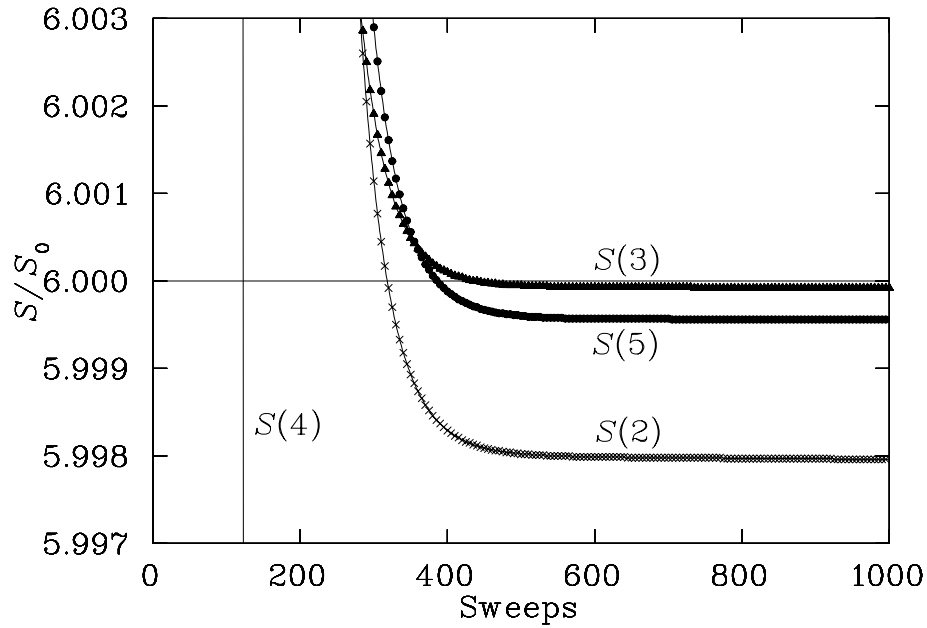


FIG. 5: Action values over the first 1000 cooling sweeps of configuration 89 cooled with the $S(2)$ (crosses), $S(3)$ (triangles), $S(4)$ (vertical line) and $S(5)$ (circle) actions. Note that $S(4)$ drops to a value near 5.00, while the other actions plateau near 6.00. [See Fig. (3) caption for notation.]

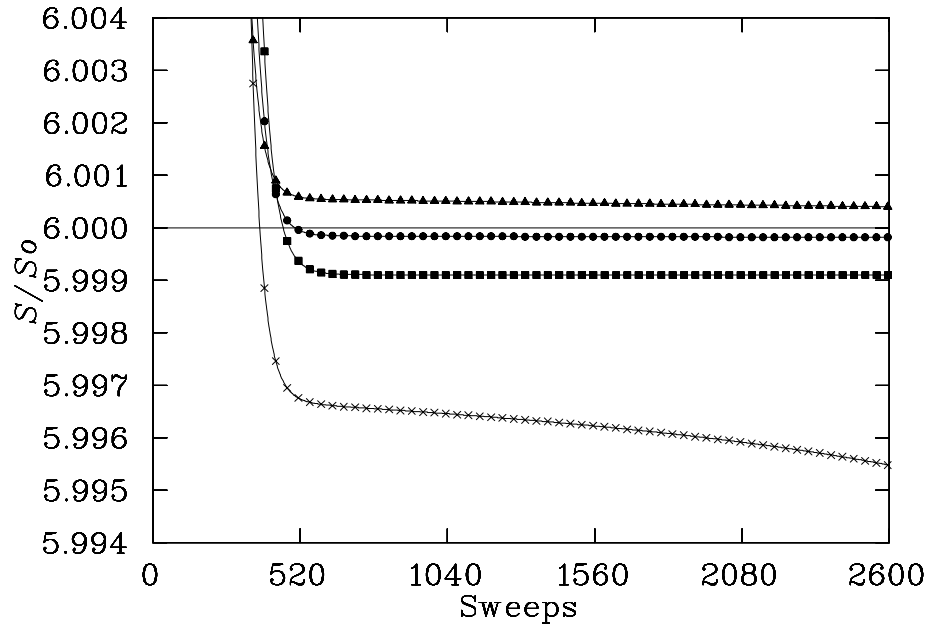


FIG. 6: Action values over the first 2600 cooling sweeps of configuration 32 cooled with (from top to bottom on the right-hand-side of the figure) $S(3)$ (triangles), $S(5)$ (circles), $S(4)$ (squares), and $S(2)$ (crosses). [See Fig. (3) caption for notation.]

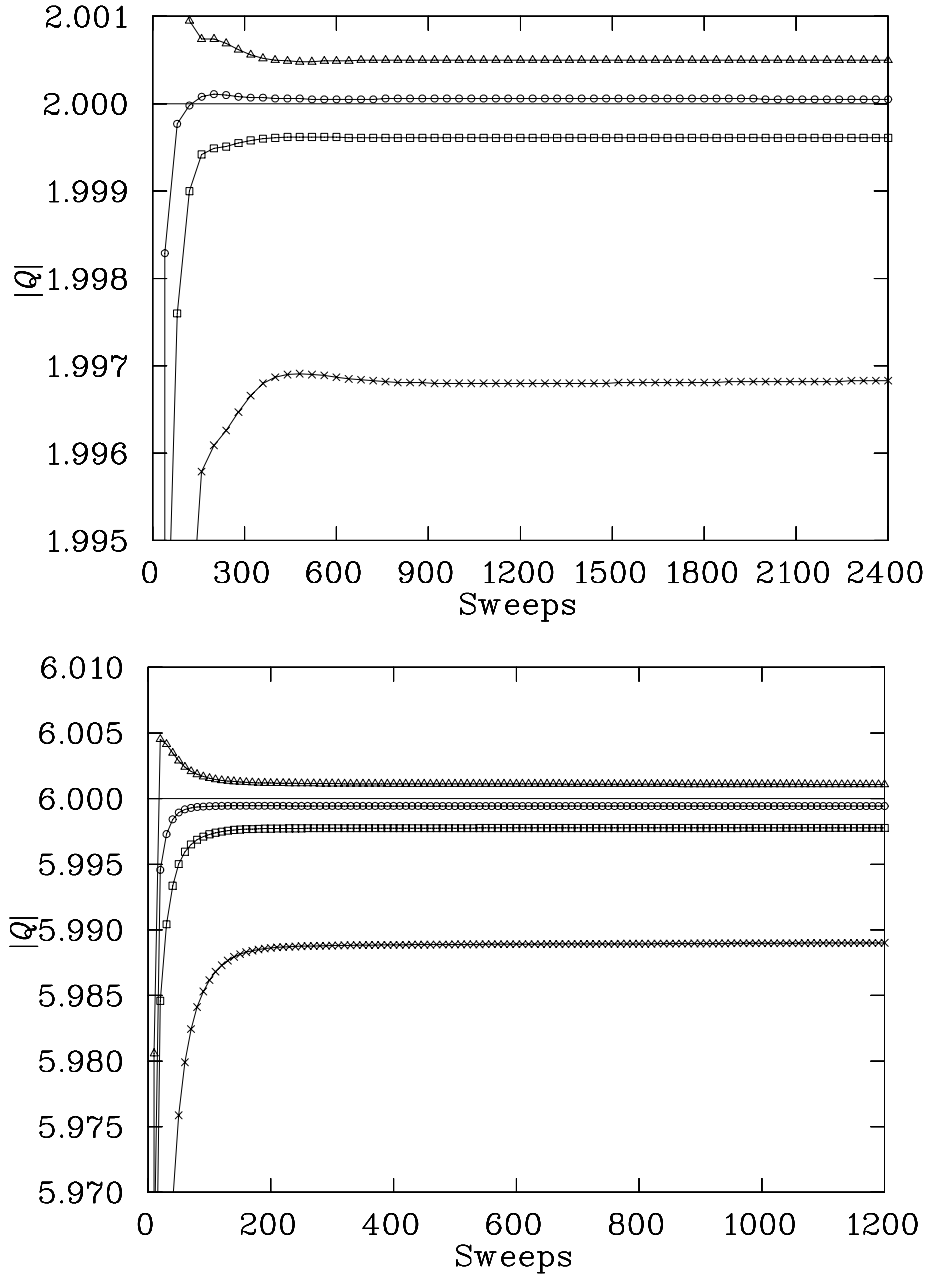


FIG. 7: Topological Charge of configuration 27 (top) and configuration 89 (bottom) cooled exclusively with the $S(3)$ cooling scheme, for 2400 sweeps and 1200 sweeps respectively. In descending order the curves are $Q(3)$, $Q(5)$, $Q(4)$, and $Q(2)$. The $Q(5)$ (circles) operator falls directly between the $Q(3)$ (triangles) and $Q(4)$ (squares) topological charge operators, at almost perfect integer values. [See Fig. (3) caption for notation.]

TABLE I: Reconstructed action (rescaled by S_0) and Q values from various configurations with $S(3)$ cooling. The columns are the configuration number, the sweep number at which the calculation was performed, the value of the cooling action, the values of $S_R(2)$ to $S_R(5)$, and the values of $Q(2)$ to $Q(5)$. [See Fig. (3) caption for notation.]

Config.	Sweep	$S(3)$	$S_R(2)$	$S_R(3)$	$S_R(4)$	$S_R(5)$
89	1071	5.99992	5.98908	6.00110	5.99777	5.99943
27	1400	2.00013	1.99687	2.00055	1.99965	2.00010
90	1046	1.99999	1.99849	2.00012	1.99978	1.99995
56	2446	1.99996	1.99878	2.00002	1.99979	1.99990

Config.	Sweep	$S(3)$	$Q(2)$	$Q(3)$	$Q(4)$	$Q(5)$
89	1071	5.99992	5.98899	6.00109	5.99777	5.99943
27	1400	2.00013	1.99680	2.00050	1.99961	2.00006
90	1046	1.99999	1.99848	2.00011	1.99977	1.99994
56	2446	1.99996	1.99878	2.00002	1.99979	1.99990

the 5-loop improved field-strength is most accurate, while the 3-loop field-strength is substantially cheaper (in a computational sense) and still produces excellent results.

Assessment of improvement in the cooling action is more difficult. It has been stated by de Forcrand *et al.* [5] that $S(5)$ cooling is most dependable and produces the best stabilization of instantons. We have cooled configurations with a topological charge of $|Q| = 2$ and have seen that the instantons rapidly settle on mutually consistent sizes, and furthermore each instanton changes size by a factor of no more than 1.1 over the course of several thousand sweeps. This work will be reported in detail elsewhere [12]. However de Forcrand *et al.*'s work establishes a precedent which must be recognized, so let us mention some differences between their work and ours. Firstly, our work is performed on configurations which contain several instantons or anti-instantons while de Forcrand *et al.*'s work is performed on configurations which consist of a single instanton, obtained via $S(1)$ cooling. Furthermore our work is performed on a 4-toroidal mesh of lattice points, with untwisted boundary conditions while de Forcrand *et al.*'s work is performed with twisted boundary conditions. The twist in the boundary conditions serves to stabilize the single instanton present, since self-dual $|Q| = 1$ configurations are not permitted on an untwisted torus [10, 11, 13].

As demonstrated in Table II, for our (periodic) lattice the $S(3)$ cooling action produces results as good as $S(5)$. $S(3)$ cooling is significantly faster than $S(5)$, since it requires fewer link multiplications, and gives no noticeable decrease in long-term instanton stability. In fact, for large numbers of cooling sweeps $S(5)$ cooling appears to consistently produce lower values of S/S_0 than $S(3)$ cooling, and lower than the required integer value, suggesting the presence of $\mathcal{O}(a^6)$ discretization errors which contribute negatively. Over the long term these errors may destabilize instantons (as was observed with $S(4)$ cooling), suggesting that

TABLE II: Reconstructed action and cooling action values (all rescaled by S_0) from various configurations cooled with $S(3)$ (columns 3 to 5) and $S(5)$ (columns 6 to 8). [See Fig. (3) caption for notation.] After no more than 170 cooling sweeps, the mean-field improvement factor u_0 for configurations 89 and 32 have settled on a value of 0.99992, and remain completely stable thereafter, while configuration 39 settles on a value of $u_0 = 0.99996$. The resultant weighting of the 3×3 loop to the 1×1 loop is $u_0^8 \approx 0.9995$.

Config.	Sweep	$S(3)$	$S_R(3)$	$S_R(5)$	$S(5)$	$S_R(3)$	$S_R(5)$
89	200	6.03297	6.03417	6.03243	6.05030	6.05190	6.05012
	600	6.00010	6.00130	5.99961	5.99957	6.00116	5.99945
	1000	5.99992	6.00110	5.99944	5.99956	6.00115	5.99945
39	220	3.12225	3.12234	3.12203	3.16616	3.16629	3.16596
	520	3.00024	3.00041	3.00013	3.00051	3.00074	3.00045
	920	2.99992	3.00009	2.99980	2.99986	3.00009	2.99980
32	500	6.00061	6.00300	5.99995	6.00000	6.00319	6.00006
	1000	6.00051	6.00284	5.99988	5.99984	6.00298	5.99990
	1500	6.00047	6.00274	5.99986	5.99983	6.00294	5.99989

$S(3)$ is the safer choice for investigations of long-term instanton stability.

VII. CONCLUSIONS

In summary, to assess the relative merits of the improvement schemes discussed in this paper, we compare the various cooling actions (rescaled by the single instanton action S_0), with reconstructed actions (rescaled by S_0) and topological charges based upon various forms of the improved field-strength tensor, $F_{\mu\nu}$. For studies of instantons on periodic (untwisted) lattices the $S(3)$ action is optimal for cooling, due to the superior accuracy with which it approaches integer values, its promise of long-term stability, and cost-effective execution. Five-loop improvement is optimal for the field-strength tensor, as most integer-like results are obtained from $Q(5)$ for the improved topological charge operator and $S_R(5)$ for the reconstructed action. However the 3-loop operator also produces excellent results, and is much less computationally demanding than the 5-loop operator. This recommends the 3-loop field-strength as a reasonable alternative choice to the 5-loop improved field-strength when computational resources are limited and improved accuracy at the order of a few parts in 10^4 is not required.

The improved field-strength tensor has already been used in a number of investigations. For example, the 3-loop topological charge described in this paper has been used to assess the Atiyah-Singer index theorem [14] on uncooled and cooled field configurations [15]. The highly-improved field-strength tensor has also been used in a “fat-link irrelevant clover” (FLIC) action [16], a modification of the Sheikholeslami-Wohlert improved quark action

[17], where the links of irrelevant operators are fattened via APE smearing. Detailed investigations of the long-term behaviour of instantons under $\mathcal{O}(a^4)$ -improved cooling have been performed [12], including investigations of the consequences of the Nahm transform [10, 13, 18] for the stability of $|Q| = 1$ configurations on the 4-torus.

Areas of future research using the improved field-strength tensor include adaptation to the study of glueball and hybrid meson spectra where colour-magnetic and electric fields explicitly provide gluonic excitations in the hadron interpolating fields [19, 20]. Future investigations should also investigate dislocation thresholds to learn how coarse the lattice can be made before a substantial reduction in the quality of data occurs.

Acknowledgements

We thank Paul Coddington and Francis Vaughan of the South Australian Centre for Parallel Computing and the Distributed High-Performance Computing Group for support in the development of parallel algorithms in High Performance Fortran (HPF). Calculations were carried out on the Orion supercomputer at the Australian National Computing Facility for Lattice Gauge Theory (NCFLGT). This work was supported by the Australian Research Council.

-
- [1] K. Symanzik *Nucl. Phys.* **B226**, 187 (1983).
 - [2] G. P. LePage *Redesigning Lattice QCD*, [hep-lat/9607076] (1996).
 - [3] F. D. R. Bonnet, D. B. Leinweber, A. G. Williams, and James M. Zanotti, *Improved Smoothing Algorithms for Lattice Gauge Theory* [hep-lat/0106023], to appear in *Phys. Rev. D* (2002).
 - [4] F. D. R. Bonnet, D. B. Leinweber, and A. G. Williams, *J. Comput. Phys.* **170**, 1 (2001).
 - [5] P. de Forcrand, M. G. Perez, I-O. Stamatescu *Nucl. Phys.* **B499**, 409 (1997).
 - [6] K. G. Wilson, *Phys. Rev.* **D10**, 2445 (1974).
 - [7] M. G. Perez, A. G.-Arroyo, J. Snippe and P. van Baal, *Nucl.Phys.* **B413**, 535-552 (1994).
 - [8] N. Cabbibo and E. Marinari, *Phys. Lett.* **B119**, 387 (1982).
 - [9] T-P. Cheng and L-F. Li, *Gauge Theory of Elementary Particle Physics*, Oxford Science Publications (1988).
 - [10] C. Taubes, *J. Diff. Geom.* **19**, 517-560 (1984).
 - [11] H. Schenk, *Comm. Math. Phys.* **116**, 177-183 (1988).
 - [12] S. O. Bilson-Thompson, G. Dunne, D. B. Leinweber and A. G. Williams (ADP-01-51/T483), to be submitted to *Physical Review D*.
 - [13] P. van Braam and P. van Baal, *Comm. Math. Phys.* **122**, 267-280 (1989).
 - [14] M.F. Atiyah, I.M. Singer, *Ann. Math.* **87**, 484 (1968); *ibid.* **93**, 119 (1971).
 - [15] J. B. Zhang, S. O. Bilson-Thompson, F. D. R. Bonnet, D. B. Leinweber and A. G. Williams, *Numerical study of lattice index theorem using improved cooling and overlap fermions* [hep-lat/0111060], to appear in *Physical Review D* (2002).

- [16] J. M. Zanotti, S. O. Bilson-Thompson, F. D. R. Bonnet, P. D. Coddington, D. B. Leinweber, A. G. Williams, J. B. Zhang, W. Melnitchouk, F. X. Lee, *Hadron masses from novel fat-link fermion actions* [hep-lat/0110216], to appear in *Physical Review D* (2002).
- [17] B. Sheikholeslami and R. Wohlert, *Nucl. Phys.* **B259**, 572 (1985).
- [18] A. Gonz'alez-Arroyo and C. Pena, *Nucl. Phys. Proc. Suppl.* **83**, 533-535 (2000).
- [19] D. Toussaint, *Nucl. Phys. Proc. Suppl.* **83**, 151 (2000).
- [20] P. Lacock, C. Michael, P. Boyle, and P. Rowland, *Phys. Rev.* **D54**, 6997 (1996).